JCTC Journal of Chemical Theory and Computation

pubs.acs.org/JCTC Article

Relationships between Orbital Energies, Optical and Fundamental Gaps, and Exciton Shifts in Approximate Density Functional Theory and Quasiparticle Theory

Yinan Shu and Donald G. Truhlar*

Cite This: J. Chem. Theory Comput. 2020, 16, 4337−4350 Read Online

ACCESS | Metrics & More | Article Recommendations

ABSTRACT: The relationships between Kohn−Sham (KS) and generalized KS (GKS) density functional orbital energies and fundamental gaps or optical gaps raise many interesting questions including the physical meanings of KS and GKS orbital energies when computed with currently available approximate density functionals (ADFs). In this work, by examining three diverse databases with various ADFs, we examine such relations from the point of view of the exciton shift of quasiparticle theory. We start by calculating a large number of excitation energies by time-dependent density functional theory (TDDFT) with a large number of ADFs. To relate the exciton shift implicit in TDDFT to the exciton shift that is explicit in Green's function theory, we define the exciton shift in TDDFT as the difference of the response shift and the quasiparticle shift. We found a strong correlation between the response shift and the amount of Hartree−Fock exchange included in the density functional, with the response shift varying between −1 and 5 eV. This range is an order of magnitude larger than the mean errors of the TDDFT excitation energies. This result suggests that, with currently available functionals, the KS or GKS orbital energies should be treated as intermediate mathematical variables in the calculation of excitation energies rather than as the energies of independent-particle reference states for quasiparticle theory.

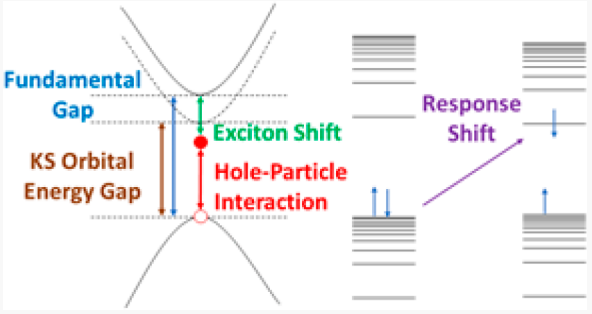

I. INTRODUCTION

The goal of the present paper is to study the interpretation of excitonic effects in time-dependent (TD) Kohn−Sham (KS) density functional theory (DFT) using approximate density functionals in common use. There is a large amount of literature on the interpretation of orbital energies in KS theory, especially their relation to ionization energies, electron affinities, and excitation energies,[1−27] and it has also been said that, "It is interesting to ask to what extent the resulting one-electron energies agree with the excited-state energies of the system calculated within quasiparticle theory."[28] In order to discuss one's expectation in this regard, it is useful to review the language and the theoretical frameworks involved. In addition to the widely employed language in the literature, e.g., optical gap, fundamental gap, etc., we relate the implicit excitonic effect in TDDFT to the *response shift* and quasiparticle shift. The definitions of various quantities used in this work and their relationships with one another are illustrated in Scheme 1. We begin by discussing the difference between two major approaches applied to the calculation of electronic excitation energies, namely, TDDFT, widely used in chemical physics, and many-body Green's function theory, widely used in condensed-matter physics. The TDDFT approach is often discussed in terms of orbitals and configuration state functions, whereas the Green's function approach is discussed in terms of quasiparticles. Excellent

Scheme 1

Quantity		Definition
OptG	optical gap	absorption threshold
FunG	fundamental gap	IP − EA
OrbG	orbital energy gap	LUMO energy − HOMO energy
HS	hole shift	IP − (−HOMO energy)
PS	particle shift	(−LUMO energy) − EA
QS	quasiparticle shift	HS+PS = FunG - OrbG
ES	exciton shift	OptG − FunG
RS	response shift	QS + ES = OptG − OrbG

Received: March 31, 2020
Published: May 26, 2020

https://dx.doi.org/10.1021/acs.jctc.0c00320
J. Chem. Theory Comput. 2020, 16, 4337−4350

technical reviews are available elsewhere.[29,30] What follows is an introduction.

In discussing the theories, we shall divide quantum mechanical electronic structure methods into two branches: density functional theory and wave function theory (WFT). In DFT, we use the Hohenberg−Kohn theorem,[31] and in this article we restrict our attention to KS-DFT,[32] in which the electron density is represented by a single Slater determinant corresponding to noninteracting electrons and to generalized Kohn−Sham[33] (GKS) theory, in which the electron density is represented by a single Slater determinant corresponding to partially interacting electrons. In contrast, WFT is the type of theory that uses the Schrödinger equation without the Hohenberg−Kohn theorems, and so WFT includes Green's function theory.

We start with KS-DFT and in particular with periodic solids, which are also called crystals. We define the orbital energy gap as the orbital energy of the bottom of the Kohn−Sham conduction band minus the orbital energy of the top of the Kohn−Sham valence band. Another way to say this is that it is the energy of the lowest unoccupied crystal orbital (LUCO) minus the energy of the highest occupied crystal orbital (HOCO). For molecules, it is the same except we have the energy of the lowest unoccupied molecular orbital (LUMO) minus the energy of the highest occupied molecular orbital (HOMO).

Returning to crystals, in KS theory, the orbital energies of the particles (i.e., excited electrons) and holes are independent-electron energies. However, when an excitation occurs, the electronic charge distribution relaxes (independent-particle states are mixed by electron−electron interactions). It is convenient, following Landau's theory of the Fermi liquid,[34] to then focus on the elementary excitations of the system and interpret them as quasiparticles.[35] This leads to the quasiparticle spectrum, formed from elementary excitations that do not interact. The difference between the gap in the quasiparticle spectrum (which is called the fundamental gap) and the independent-particle gap (orbital energy gap) is called the quasiparticle shift, and it may be several eV for local exchange-correlation functionals. A key element of quasiparticle theory is the existence of a "noninteracting system" that "is presumably now the IPA [independent-particle-approximation] in which the Coulomb interactions between electrons are treated in the mean field approximation";[36] the actual states of the system are connected to the reference states by an adiabatic connection or by perturbation theory. It is now conventional to regard the KS states or GKS states for the ($N \pm 1$)-particle system (where N is the number of electrons) as the reference IPA states for Green's function perturbation theory. One should keep in mind that the KS orbital eigenvalues depend on how the effective potential is treated in the Kohn−Sham equations;[22,37] in the present article, we use the conventional KS and GKS definitions, the former for local, orbital-independent functionals and the latter for nonlocal and/or orbital-dependent functionals (for local, orbital-independent functionals the KS and GKS orbital energies, defined in the conventional way, are the same).

The elementary excitations are of two kinds: a particle added to a system and a hole corresponding to an electron removed from a system. A quasielectron may be considered to be a combination of the added particle and the polarization it induces in its environment, and a quasihole may be considered to be the combination of the hole and the polarization it induces in its environment. (The environment is the rest of the crystal or the rest of the molecule.) The quasiparticle spectrum is thus appropriate for interpreting photoemission (removal of an electron) and inverse photoemission (addition of an electron) experiments. (For molecules, photoemission experiments are usually called photoelectron spectroscopy.) In these experiments an electron is removed from or added to a neutral system, changing its charge. The quasiparticle gap (fundamental gap) is equal to the difference between the ionization potential (IP) and the electron affinity (EA). Optical spectroscopy at energies below the work function (the analogue for molecules is below the IP) involves bound-state-to-bound-state transitions without changing the charge. Such bound−bound transitions require an additional consideration as discussed next.

Given the unknown exact exchange-correlation functional, the quasiparticle spectrum would provide a good approximation to the true states of the neutral system (and hence to the optical spectrum) for completely delocalized particles and holes, which have negligible interaction, and it would also be a reasonably good approximation for Mott−Wannier excitons, in which the particle and the hole are bound so weakly that their average distance is much greater than the size of a unit cell.

However, in some cases, the particle and the hole sit on the same site. This is called a Frenkel exciton. In this case there may be states at much lower energies (up to a few eV lower) than the quasiparticle gap. The difference of the true state energies from those in the quasiparticle approximation is called an exciton shift, excitonic effect, or exciton binding energy. Exciton shifts are of the order of magnitude of an eV for Frenkel excitons but of the order of magnitude of 0.01−0.1 eV for Mott−Wannier excitons. When we compare the fundamental gap to the gap determined as a threshold in a charge-conserving excitation as observed in the optical absorption or reflection spectrum or photoluminescence,[38] we must take account of both the quasiparticle shift and the exciton shift. The two types of excitons, Mott−Wannier exciton and Frenkel exciton, may coexist in the spectrum of a crystal, for example, in solid argon. When one considers molecules, the particle and hole are usually close enough to interact strongly, and large exciton shifts may be expected.

In solid-state physics, one typically calculates the quasiparticle shift by one or another version of GW theory[39−41] (where G denotes a single-particle Green's function[42−44] and W denotes the screened Coulomb interaction), and this takes one out of the realm of DFT into WFT. The foundation for the GW approximation is Dyson's equation[45−47] involving the interacting one-particle Green's function, the noninteracting one-particle Green's function, and the self-energy, which is the potential operator that generates a quasielectron or quasihole and the elementary detachment and attachment energies. (The self-energy may be distinguished from the Kohn−Sham exchange-correlation potential that generates the ground-state density and the ground-state energy.) The GW method approximates the self-energy by a physically motivated expansion of the self-energy in terms of a screened Coulomb potential and one-electron Green's function, and this can lead either to one-shot calculations or to iterative ones. Usually Kohn−Sham orbitals are used to provide a starting point for the GW calculations. There is no reason why the initial guess for the iterations must come from Kohn−Sham theory, i.e., one may use Hartree−Fock orbitals as was done in early GW calculations,[48,49] but the similarity of the physical interpreta-

https://dx.doi.org/10.1021/acs.jctc.0c00320
J. Chem. Theory Comput. 2020, 16, 4337−4350

tions of the Kohn−Sham potential and the self-energy makes the use of Kohn−Sham orbitals seem reasonable[29] (and the effective perturbation added to KS orbitals might be smaller than that added to Hartree−Fock orbitals, although one might also argue that using the Hartree−Fock orbitals would be more theoretically consistent). In practical nonconverged calculations, especially in noniterative calculations, the results of GW calculations have been found to depend strongly on the starting orbitals.

For higher accuracy, but at higher cost, one can add the so-called vertex corrections to GW calculations, and this yields what are sometimes called GWΓ calculations. The literature contains a variety of levels of GW calculations, with or without Γ, with full, partial, or no self-consistency. In the present article, we will consider non-self-consistent G_0W_0 calculations based on PBE orbital energies and screening potentials; such calculations are well-known to depend on the input data, but it is beyond our scope to examine that dependence; we do note though that the PBE starting point is a common one in the literature.

The above discussion summarizes how the quasiparticle energies are associated with non-neutral processes associated with adding or removing an electron, e.g., photoemission spectra and their inverse. For optical spectra (neutral excitations), including Wannier or Frenkel excitons or most molecular excitations, one should include the exciton shift, i.e., the interaction of the excited electron (particle) with the hole. This can be done by using the Bethe−Salpeter equation (BSE),[50−54] which involves the two-particle Green's function and most often takes the quasiparticle energies and KS wave functions as input. This is justified by the assumption that KS orbitals and quasiparticle wave functions are close to each other; this is often but not always the case. We will define the optical gap as the threshold for optical absorption, and the exciton shift is then equal to the difference between the optical gap and the fundamental gap.

A complication of the above picture is that some systems cannot be well described by perturbation theory starting from a Slater determinant and/or their excitations cannot be adiabatically connected to a single independent-electron excitation that forms a good reference state. Such systems cannot be well described by quasiparticle theory, although their total energies would still be given exactly by Kohn−Sham theory with the unknown exact density functional. Such systems are variously called strongly correlated or multireference systems, where the latter term refers to the need for reliable WFT calculations to generate them from a multiconfigurational reference state (where a configuration is a way to assign occupancies to single-particle orbitals). Systems for which quasiparticle theory is valid are called "normal Fermi systems".[55]

When one includes nonlocal Hartree−Fock exchange in the exchange-correlation functional (leading to what is usually called a hybrid functional in KS-DFT), the situation is conceptually different than the above, and it is best justified by GKS theory formulated using a partially interacting-electron reference function as opposed to the Kohn−Sham non-interacting-electrons reference function.[33]

The above discussion is an attempt to explain the main framework for considering and discussing electron excitations in solid-state physics, with a few side remarks about molecules. The mindset is somewhat different in chemical physics and physical chemistry, as discussed next. When one deals with an isolated molecule, all excitations have large electron−hole interactions, and the framework of starting with the fundamental gap and then correcting the fundamental gap for excitonic effects, is not usually considered to be the best route toward an accurate result. For molecules there are other possibilities such as converged WFT calculations by configuration interaction (CI), coupled cluster (CC) theory, or quantum Monte Carlo (QMC). The CI, CC, QMC, BSE, KS, and GKS options can all in principle be exact for electronic excitation energies, although in practice one is limited by the enormous (usually impractical) computational requirements of a converged wave function calculation by BSE, CI, CC, or QMC (although great progress has been made for smaller molecules[56,57]). So one turns again to DFT-based approaches, but rather than follow up a KS calculation with a GW or GWΓ calculation followed by a BSE calculation, the more popular approach in chemical physics is time-dependent density functional theory, which treats the electromagnetic field of the incident light as a time-dependent potential and uses the fact that the response of the ground state to the perturbation by this field has poles at the frequencies corresponding to excitation energies. This would be exact if the response were calculated exactly and if one used the exact, frequency-dependent exchange-correlation potential.[58−60] In practice though, one almost always just treats the linear portion of the response and uses the adiabatic approximation in which the exchange-correlation potential is a ground-state frequency-independent approximation. Even supposing one has a good approximation to the exact required exchange-correlation functional, TDDFT would get to the correct answer in quite a different way than the GW-BSE approach; for example, it does not separate the quasiparticle shift from the exciton shift.

In our work, we label the sum of the quasiparticle shift and the exciton shift as the response shift, and we note that TDDFT calculates the response shift without dividing it into these two components. One way to divide it for molecular systems it would be to carry out separate KS or GKS self-consistent field calculations on the cation and the anion; this would yield the fundamental gap including the relaxation effects, and hence it would be a way to calculate the quasiparticle shift without the exciton shift, but (for reasons discussed in the next section) we shall not purse this approach in the present article, which is concerned with TDDFT.

Studying the response shift is in part supported by the desire to develop better functionals. For solids, one approach to obtaining improved density functionals is to make the percentage of Hartree−Fock exchange equal to the reciprocal of the local dielectric constant; however, one should keep in mind that the dielectric constant is a macroscopic quantity, and the use of a local dielectric constant is a model.[61] Another approach is to set minus the HOMO energy equal to the IP, which is supported by the IP theorem,[8] but this is complicated by the derivative discontinuity in the exact exchange-correlation functional of KS theory.[25,62] Since we do not have access to the exact exchange-correlation functional, it is hard to get agreement for both the fundamental gap and all the various kinds of excitation energies (for example, to develop an exchange-correlation functional that is equally accurate for valence, Rydberg, and charge-transfer neutral excitations as well as for IPs and EAs), but the goal is to make such properties as accurate as possible for as broad a class of systems as possible, while, at least ideally, keeping good accuracy for other aspects of energy prediction.[63] For example, photochemical dynamics requires not just good accuracy for vertical

https://dx.doi.org/10.1021/acs.jctc.0c00320
J. Chem. Theory Comput. 2020, 16, 4337−4350

Table 1. Local Functionals and Global-Hybrid Functionals Considered in the Current Work and Their Corresponding Percentages of Hartree−Fock Exchange

functional	ref	X^a	functional	ref	X	functional	ref	X
B3LYP	103,104	20	B97	105	19.43	B97M-rV	106	0
B97M-V	107	0	BHHLYP	104, 108	50	GAM	109	0
GVWN5	110,111	0	HCTH407	112	0	HLE16	113	0
M05	114	28	M05-2X	115	56	M06	70	27
M06-2X	70	54	M06-HF	116	100	M06-L	117	0
M08-HX	118	52.23	M08-SO	118	56.79	M11-L	119	0
MN12-L	120	0	MN15	121	44	MN15-L	122	0
MPW1B95	123	31	MPW1LYP	124	25	MPW1PBE	124	25
MPW1PW91	124	25	MPWB1K	123	44	N12	126	0
O3LYP	104, 127	11.61	OLYP	104, 128	0	PBE	73	0
PBE0	125, 129	25	PBE50	130	50	PW91	131	0
revPBE0	132	25	revTPSS	133	0	revTPSSh	134	10
SOGGA11-X	135	40.15	GPW92	110, 136	0	τ-HCTH	137	0
τ-HCTHh	138	15	TPSS	139	0	TPSS0	138	25
TPSSh	140	10	X3LYP	104, 141	21.8			

$^a X$ is the percentage of Hartree−Fock exchange.

excitation energies but also broad accuracy in predicting the topographies of the potential energy surfaces, including bond energies, barrier heights, noncovalent interactions, and electrostatic interactions. One experimentally accessible property that has not been well utilized in developing density functionals is the exciton shift.

To assess the excitonic effect in TDDFT, we are trying to answer the following questions: (1) What response shift is required in TDDFT with various functionals? (2) Are there functionals in common use for which the calculated orbital energy gap matches well with the fundamental gap or optical gap?

We close the introduction with two final comments. First, we remind the reader that in the generalized Kohn−Sham theory, i.e., when one is using functionals with a nonzero portion of Hartree−Fock exchange, there is not a single exact functional, but rather there is a different exact functional for every different percentage of Hartree−Fock exchange.[9,64] Second, we stress that we are intentionally not using any theorems about the unknown exact functionals nor are we entering the debates[3,18,27] about the implications of Janak's theorem[2] or the IP theorem.[8] Instead, a goal of the present article is to test whether it is reasonable to assume that KS states are reasonably interpreted as reference IPA states for quasiparticle theory when one uses currently available approximate density functionals to compute the KS states. We intentionally avoid attributing our findings to the "true" KS states that would be obtained with an unknown exact density functional, as these may be different to varying degrees from the KS states obtained with the presently used approximate functionals.[4,65]

II. DATA SETS AND COMPUTATIONAL DETAILS

Three data sets are considered in the current work. One, called VT28,[66,67] consists of three vertical transition energies each for 28 small organic molecules, for a total of 84 test cases. The geometries are obtained from ref 66, which are ground-state equilibrium geometries optimized by Møller−Plesset second-order perturbation theory[68] (MP2) with the 6-31G*[68] basis set. With these geometries, vertical excitation energies were calculated by TDDFT calculations with the 6-311+G(2df,p) basis set and various exchange-correlation functionals. For each molecule in this data set, we consider the three singlet excited states whose dominant excitation characters are HOMO → LUMO, HOMO − 1→ LOMO, and HOMO → LUMO + 1.

The second data set, called VT160,[69] consists of two vertical transition energies each for 80 diverse medium-sized and large molecules (called "real-life compounds" in ref 69). The molecules include, for example, hydrocarbons, dyes, fluorophores, inorganic compounds, and transition metal complexes, cations. The two transition energies for each molecule are the singlet vertical excitations whose dominant excitation character is HOMO → LUMO at two geometries, which correspond to the minimum energy of the ground state and that corresponding to the minimum of the excited state as optimized by KS-DFT and TDDFT, respectively, with the M06-2X[70] exchange-correlation functional and the 6-31+G(d)[68] basis set. (These geometries are given in the Supporting Information of ref 69.) Hence there is a total of 160 geometries. With these geometries, KS-DFT and TDDFT calculations were performed with the def2-TZVPP[71] basis set and various exchange-correlation functionals.

The third data set, called GW100,[72] consists of 100 diverse molecules that include diatomic metal compounds, small metallic clusters, alkaline metal halides, alkaline earth metal compounds, and organic molecules. These molecules cover a wide range of excitation energies and IPs. The geometries are taken from ref 72, where they were obtained either from experiment or optimized by KS-DFT with the PBE functional[73] and the def2-QZVP[71] basis set. For comparison, we calculated vertical excitation energies were calculated by TDDFT with the def2-QZVP basis set and various exchange-correlation functionals. For each molecule, the data set includes one singlet excited state whose dominant character is HOMO → LUMO.

The functionals considered in the current work and their corresponding percentages (X) of Hartree−Fock exchange (Hartree−Fock exchange) are summarized in Table 1.

All calculations are performed with *Q-Chem 4.4*.[74] All calculations are carried out in the framework of KS theory[32] for local density approximations and gradient approximations and by GKS theory[9] (rather than by using an optimized effective potential[75]) for orbital-dependent functionals. Note that KS theory and GKS theory are the same for local density

https://dx.doi.org/10.1021/acs.jctc.0c00320
J. Chem. Theory Comput. 2020, 16, 4337−4350

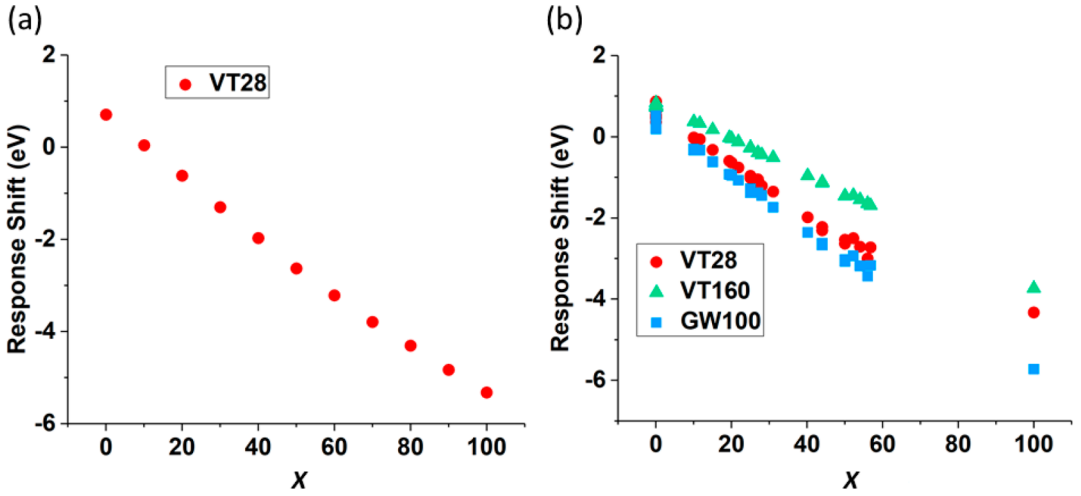

Figure 1. Response shift as a function of the percentage of the Hartree−Fock exchange employed in the functionals. (a) PBE*X* functionals with the VT28 data set. (b) Functionals listed in Table 1 with the VT28, VT160, and GW100 data sets. Each point in the plots represents the average response shift for a given functional.

approximations and gradient approximations. For orbital-dependent functionals, though, the distinction is important because although the total energies are the same with the GKS and optimized effective potential formulations, the orbital energies are different. The response shifts are computed in the present article by using adiabatic TDDFT with the Tamm−Dancoff approximation,[76] which will simply be called TDDFT in the rest of the article. (Our general experience is that the conclusions would not be significantly different if we used the full linear response instead of the Tamm−Dancoff approximation.)

III. RESULTS AND DISCUSSION

In discussing the results for molecules, we will use the language in Scheme 1. Note that for crystals, the IP becomes the work function, the orbital gap becomes the band gap, the HOMO becomes the HOCO (valence band maximum), and the LUMO becomes the LUCO (conduction band minimum). Notice that the hole shift and particle shift are defined in such a way that the quasiparticle shift can be written as their sum.

III.A. Response Shift of TDDFT. First, we investigated the response shift of TDDFT for the data set VT28 by using a series of exchange-correlation functions called PBE*X* functionals. A PBE*X* functional is defined as starting with the local PBE functional and replacing the X percentage of local exchange by the Hartree−Fock exchange with no other changes. Notice that the standard PBE50[130] functional is the same as PBE*X* with $X = 50$, and the standard PBE0[125,129] functional (also sometimes called PBE1PBE) is the same as PBE*X* with $X = 25$. In the current work, we consider X values ranging from 0 to 100 with 10 as the increment size.

Panel a of Figure 1 shows the response shift of TDDFT as a function of the percentage of the Hartree−Fock exchange in the PBE*X* functional. Each dot in the scatter plot represents the average response shift over the 28 data for one functional plotted vs that functional's value of X. The plot shows that the percentage of the Hartree−Fock exchange has a strong influence on the response shift. For $X \approx 10$, the orbital energy gap is very close to the optical gap; the equality of these gaps corresponds to a zero response shift.

Panel b of Figure 1 shows the response shift of TDDFT for data sets VT28, VT160, and GW100 for the functionals of Table 1. The exchange-correlation functionals in Table 1 involve a great variety of local exchange and correlation components, so we might expect to find a weaker correlation between the response shift and percentage of Hartree−Fock exchange in panel b than we found in panel a, where the Hartree−Fock exchange was systematically replacing a percentage of the local exchange with all other aspects of the functional held fixed. Surprisingly, though, the correlation in panel b remains strong and dramatic for all three databases. This indicates that the percentage X of Hartree−Fock exchange is by far the most important element in the size of the predicted response shift. A linear regression line fitted to all three data sets passes through zero at 9.7% Hartree−Fock exchange.

The individual data point comparisons for the correlation of the optical gap with the orbital energy gap are shown in Figure 2 for three popular functionals, PBE, B3LYP, and M06-2X. These functionals have percentages of Hartree−Fock exchange equal to 0, 20, and 54, respectively. The results in Figure 2 are consistent with Figure 1 in that for local functionals (which have the percentage of Hartree−Fock exchange equal to zero), the orbital energy gap tends to systematically underestimate the predicted excitation energy, leading to a positive predicted response shift, and as X increases, the excitation energy for a given orbital energy gap tends to get lower.

From Figure 1, we know that the variation in response shifts due to the change in percentage of the Hartree−Fock exchange is very large; the average response shift can change by more than 5 eV as one progresses from local functionals ($X = 0$) to functionals with 100% of Hartree−Fock exchange. This is especially striking if it is considered in the context of Figure 3, which compares the TDDFT and BSE excitation energies for the data set VT160, where the BSE ones are considered to be accurate reference values. This comparison indicates that the TDDFT excitation energies are close to those of BSE, usually within 0.4 eV. We conclude that the huge variation in the response shifts must be canceling out wide variations in the orbital energy gap so that the optical gaps come out reasonable.

III.B. Quasiparticle Shift of TDDFT. One complication of analyzing the shifts is that a Kohn−Sham functional might be designed such that the HOMO orbital energy equals the exact

https://dx.doi.org/10.1021/acs.jctc.0c00320
J. Chem. Theory Comput. 2020, 16, 4337−4350

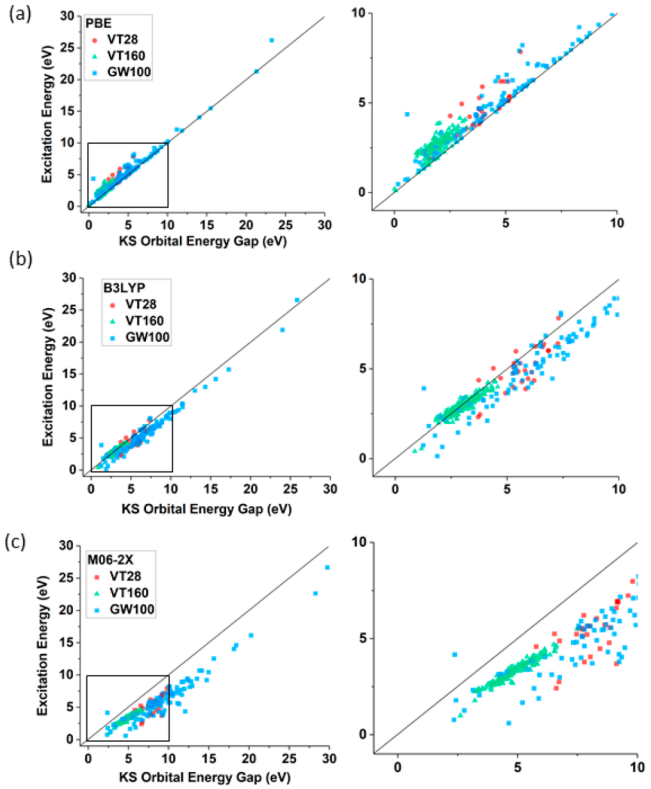

Figure 2. Response shifts for the VT28, VT160, and GW100 data sets: (a) PBE, (b) B3LYP, and (c) M06-2X. Each panel on the left has 288 dots representing each of the comparisons without averaging. The three panels on the right are zoomed in for the energy range from 0 to 10 eV, which is outlined by a square in the left-side panels. Each panel has a line at 45 deg to guide the eye in interpreting the correlation.

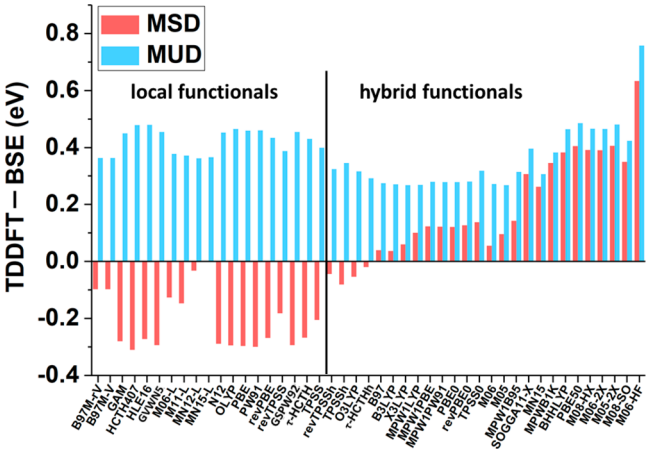

Figure 3. Mean signed deviation (MSD) and mean unsigned deviation (MUD) between TDDFT and BSE excitation energies of the VT160 data set. The hybrid functionals arranged in order of increasing percentage of Hartree−Fock exchange.

ionization potential (such a procedure is motivated by the theorem,[8] and such functionals have been called optimally tuned hybrids[20]), then the GW correction to the ionization potential should be zero. However, most approximate functionals have not been designed this way, and our goal here is to examine the systematic trends in currently available density functionals in the language of Scheme 1.

Strictly speaking, we are not computing the quasiparticle shift. Instead, we are computing the quasiparticle shift that would be needed to make the density functional give an accurate fundamental gap. This is because the response in TDDFT cannot simply be separated into a quasiparticle shift and an exciton shift as in BSE. Within the realm of DFT, one may in fact compute the "true" quasiparticle shift (or hole shift or particle shift) in various ways. These methods include (a) computing the excitation energies of ionized states by TDDFT, (b) computing the differences of KS-DFT ground state energies for the neutral, cationic, and anionic species (this method is usually denoted as ΔSCF in the literature), and (c) employing a Koopmans-like approach that does not allow orbital relaxation. Method a is impractical because there are an infinite number of Rydberg states below the first ionized state. Method b is in fact employed in practical calculations, but there are complications. For example, anions might be unbound for small molecules when using local functionals. Another issue is that the excitation energies of bound states computed by ΔSCF are not the same as those computed by TDDFT, so for consistency one should compare IPs computed by ΔSCF to excitation energies computed by ΔSCF, but ΔSCF excitation energies can usually be computed only when the excited state has a different symmetry than the ground state. Method c is inconsistent with TDDFT because excited states in TDDFT can use the ground-state virtual orbitals, where Koopmans' ions cannot.

In this section, we therefore employ an indirect scheme; we approximately assess the quasiparticle shift by comparing the magnitudes of the HOMO and LUMO orbital energies with IPs and EAs. This provides estimates of what hole shift, particle shift, and quasiparticle shift would be required by each functional to get the experimental IPs and EAs starting with that functional's orbital energies.

For this purpose, we compare the magnitudes of the HOMO and LUMO orbital energies to the experimental data for IPs and EAs in ref 72. The experimental data covers 97 IP data and 26 EA data. The required hole shift averaged over the 97 data points and the required particle shift averaged over 26 data points are shown in Figure 4. The required quasiparticle shift is computed by addition of the required hole shift and particle shift. Linear regression on this data suggest that the required hole shift, particle shift, and quasiparticle shift reach 0 for functionals with a Hartree−Fock exchange around 82%, 82%, and 83%, respectively. This seems to indicate that one could obtain density functionals whose frontier orbital energies give the IP and EA if one optimized functionals with X in the range 80−85%, which reflects some trends already available in the literature.[20,26,77,78] Hybrid functionals employing an amount of Hartree−Fock exchange equal to the inverse of a dielectric constant have suggested a larger X is required for larger band gap semiconductors due to stronger electronic screening.[61,79−86] Molecules, most of which have large fundamental gaps, are in some sense close to large band gap semiconductors, and this may help to understand why a large X is required.[87] However, the better accuracy for IPs with very large X may reflect a cancellation of errors since raising X so high can lower the accuracy of other predictions.[88] A more physical solution may require the use of range-separated hybrid functionals (with high X at large interelectronic separation and lower X at smaller interelectronic separation), as considered further below.

https://dx.doi.org/10.1021/acs.jctc.0c00320
J. Chem. Theory Comput. 2020, 16, 4337−4350

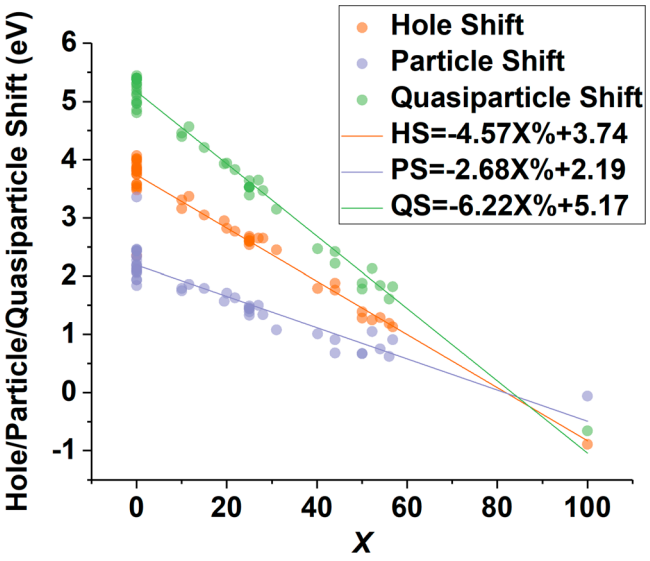

Figure 4. Hole shift, particle shift, and quasiparticle shift predicted by combining the orbital energies of the functionals listed in Table 1 with the experimental data in ref 72.

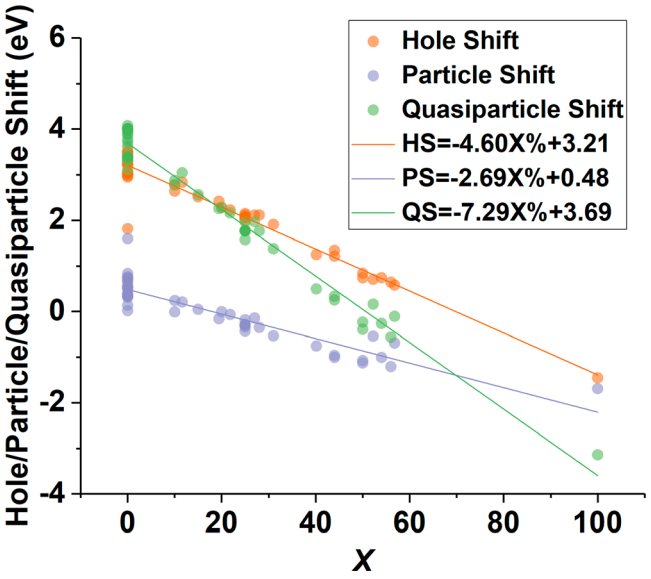

Figure 5. Hole shift, particle shift, and quasiparticle shift predicted by combining the orbital energies of the functionals listed in Table 1 with G_0W_0 results (GW/AIMS-P16 data from the GW100 data set) of ref 72.

An alternative way to interpret Figure 4 is that one is combining experimental data with independent-particle orbital energies to predict the polarization effects that constitute the hole shift, particle shift, and quasiparticle shift. With that interpretation, we see that different density functionals give widely different predictions, and if we accepted this interpretation, we would conclude that they model ionization and attachment with very different physical pictures.

Another way to assess the quasiparticle gap of TD-DFT is to compare to the G_0W_0 results of ref 72; in particular, we compare to the G_0W_0 results denoted as AIMS-P16 in ref 72. (The AIMS-P16 data cover the whole GW100 data set.) We compare minus the HOMO energy to the G_0W_0 IP, minus the LUMO energy to the G_0W_0 EA, and the orbital energy gap to the G_0W_0 fundamental gap. Since the goal of GW theory is to convert the orbital energies into quasiparticle energies, this would be a direct measure of the required quasiparticle gaps if G_0W_0 were accurate. Reference 72 shows that, although there are some significant quantitative errors, there does exist a rough correlation of the G_0W_0 predictions with the IPs and EAs. Therefore, the comparison is interesting, and it is shown in Figure 5. One sees strong correlation between the required hole, particle, and quasiparticle shifts and the percentage of Hartree−Fock exchange in the functionals. The linear regression in Figure 5 for the whole shift is close to that computed from experimental results in Figure 4, but the linear regression of the particle shift is very different, although they have similar slopes. The linear regressions in Figure 5 indicate that the required hole shift, particle shift, and quasiparticle shift for DFT orbital energies to match the G_0W_0 quasiparticle energies reach 0 for functionals with X of 70%, 18%, and 51%, respectively. Therefore, in order to obtain orbitals whose HOMO and LUMO energies are close to the (negatives) of the G_0W_0-predicted IPs and EAs, very different percentages of Hartree−Fock exchange would be required in the functionals.

Table 2 presents the mean signed error (MSE) and mean unsigned error (MUE) of the G_0W_0 calculations of ref 72 from the experimental IPs, EAs, and FunGs. (There are 97 experimental IPs, 26 experimental EAs, and 23 experimental fundamental gaps in the GW100 data set.) The MSEs of the G_0W_0 calculations for IP, EA, and FunG are 0.59, 1.76, and 1.23 eV, respectively.

Table 2 also compares the KS and GKS orbital energies to the same experimental data. The deviations from the experimental data are labeled as errors for the G_0W_0 calculations because those calculations are supposed to yield quasiparticle energies. However, for the KS and GKS calculations, they are labeled as deviations, and the signed deviations are defined such that they have the meaning of hole shifts, particle shifts, and quasiparticle shifts. In addition to the functionals listed in Table 1, Table 2 also includes additional range-separated functionals, namely, CAM-B3LYP,[89] HSE-HJS,[90,91] M11,[92] MN12-SX,[93] N12-SX,[93] ωB97,[94] ωB97M-V,[95] ωB97X,[94] ωB97X-D,[96] ωB97X-D3,[97] ωB97X-rV,[98] ωB97X-V,[99] and ωM06-D3.[97] Examining this table shows that in some cases, the KS or GKS orbital energies are closer to experimental IPs, EAs, and fundamental gaps than are the G_0W_0 quasiparticle energies. In particular, for IPs, although none of the local and global-hybrid orbital energies are closer than G_0W_0 to experiment, seven of the range-separated functionals do achieve this. For EAs, there are many global-hybrid and range-separated functionals whose orbital energies are more accurate than the predictions of G_0W_0. For the FunGs, one global-hybrid (M06-HF) and many range-separated hybrid functionals have orbital energies that predict the gap more accurately than G_0W_0 quasiparticle calculations. Furthermore, there are several range-separated hybrid functionals that have smaller MUDs for all three quantities (IP, EA, and FunG) than the MUE of G_0W_0. Among these range-separated hybrid functionals, M11 has the smallest MUD of IP (0.42 eV), ωB97X-D has the smallest MUD of EA (0.65 eV), and ωB97X-D3 has the smallest MUD of the fundamental gap (0.63 eV). (We note that we have not tested optimally tuned functionals.)

A negative quasiparticle shift corresponds to greater relaxation in the cation than the anion, which seems reasonable since the added electron in the anion is often held only weakly. Therefore, it is encouraging that the MSD column for the

https://dx.doi.org/10.1021/acs.jctc.0c00320
J. Chem. Theory Comput. 2020, 16, 4337−4350

Table 2. Mean Unsigned and Signed Errors of G_0W_0/AIMS-P16 Quasiparticle Energies as Compared to Experimental Data and Mean Unsigned and Signed Deviations of KS and GKS Orbital Energies from the Same Experimental Data[a]

methods	IP (HS)		EA (PS)		FunG (QS)	
	Quasiparticle Calculations					
	MUE	MSE	MUE	MSE	MUE	MSE
G_0W_0	0.59	0.50	1.76	−1.57	1.23	−0.64
	Local and Global-Hybrid Functionals					
	MUD	MSD	MUD	MSD	MUD	MSD
B3LYP	2.87	2.82	1.71	1.71	3.94	3.94
B97	2.99	2.95	1.57	1.57	3.93	3.93
B97M-rV	3.60	3.58	2.08	2.08	4.97	4.97
B97M-V	3.61	3.58	2.08	2.08	4.97	4.97
BHHLYP	1.42	1.39	0.87	0.67	1.88	1.88
GAM	4.04	4.01	2.12	2.12	5.31	5.31
HCTH407	3.79	3.75	2.43	2.43	5.38	5.38
HLE16	2.41	2.35	3.36	3.36	5.11	5.11
LDA	3.84	3.8	2.46	2.46	5.40	5.4
M05	2.71	2.65	1.34	1.34	3.47	3.47
M05-2X	1.24	1.19	0.81	0.62	1.61	1.61
M06	2.69	2.65	1.50	1.50	3.65	3.65
M06-2X	1.34	1.29	0.90	0.75	1.84	1.84
M06-HF	0.97	−0.89	0.84	−0.06	1.01	−0.66
M06-L	3.85	3.84	1.84	1.84	5.01	5.01
M08-HX	1.30	1.25	1.15	1.05	2.13	2.13
M08-SO	1.19	1.13	1.03	0.91	1.82	1.82
M11-L	3.50	3.48	2.43	2.43	5.26	5.26
MN12-L	3.56	3.54	2.01	1.94	4.86	4.86
MN15	1.91	1.88	0.97	0.91	2.42	2.42
MN15-L	3.52	3.51	1.94	1.94	4.81	4.81
MPW1B95	2.45	2.45	1.12	1.08	3.15	3.15
MPW1LYP	2.73	2.68	1.49	1.49	3.64	3.64
MPW1PBE	2.64	2.6	1.44	1.44	3.53	3.53
MPW1PW91	2.63	2.59	1.46	1.46	3.53	3.53
MPWB1K	1.76	1.76	0.78	0.68	2.22	2.22
N12	4.06	4.02	2.19	2.19	5.38	5.38
O3LYP	3.41	3.37	1.86	1.86	4.57	4.57
OLYP	4.11	4.07	2.16	2.16	5.44	5.44
PBE	3.97	3.94	2.27	2.27	5.38	5.38
PBE0	2.65	2.61	1.44	1.44	3.53	3.53
PBE50	1.32	1.28	0.82	0.67	1.78	1.78
PW91	3.92	3.88	2.34	2.34	5.40	5.40
	Local and Global-Hybrid Functionals					
	MUD	MSD	MUD	MSD	MUD	MSD
revPBE	4.03	3.99	2.19	2.19	5.38	5.38
revPBE0	2.69	2.65	1.39	1.39	3.53	3.53
revTPSS	3.87	3.84	2.06	2.06	5.14	5.14
revTPSSh	3.35	3.31	1.75	1.75	4.40	4.40
SOGGA11-X	1.83	1.79	1.04	1.01	2.47	2.47
SPW92	3.84	3.80	2.45	2.45	5.40	5.40
τ-HCTH	3.79	3.75	2.34	2.34	5.31	5.31
τ-HCTHH	3.09	3.05	1.79	1.79	4.21	4.21
TPSS	3.89	3.86	2.11	2.11	5.20	5.20
TPSS0	2.58	2.54	1.33	1.33	3.39	3.39
TPSSh	3.48	3.16	1.79	1.79	4.46	4.46
X3LYP	2.81	2.77	1.63	1.63	3.83	3.83
	Functionals with Range-Separated Screened Exchange					
	MUD	MSD	MUD	MSD	MUD	MSD
HSE-HJS	3.04	3.01	1.80	1.80	4.26	4.26
MN12-SX	2.91	2.87	2.09	2.09	4.54	4.54
N12-SX	3.09	3.06	1.77	1.77	4.30	4.30
	Functional with Range-Separated Exchange Increasing to 65% at Long Range					
	MUD	MSD	MUD	MSD	MUD	MSD
CAM-B3LYP	1.30	1.26	0.79	0.58	1.51	1.51
	Functionals with Range-Separated Exchange Increasing to 100% at Long Range					
	MUD	MSD	MUD	MSD	MUD	MSD
M11	0.42	0.16	0.80	−0.10	0.75	−0.03
ωB97	0.43	0.10	0.88	−0.59	0.82	−0.65
ωB97M-V	0.54	0.41	0.73	−0.25	0.66	−0.05
ωB97X	0.49	0.32	0.78	−0.44	0.69	−0.33
ωB97X-D	0.86	0.80	0.65	−0.16	0.65	0.33
ωB97X-D3	0.62	0.53	0.73	−0.33	0.63	−0.05
ωB97X-rV	0.49	0.31	0.79	−0.42	0.69	−0.31
ωB97X-V	0.49	0.31	0.79	−0.42	0.69	−0.31
ωM06-D3	0.44	0.24	0.95	−0.62	0.77	−0.53

[a]All values are in the units of eV.

fundamental gap in Table 2 is negative for all the functionals for which the percentage of Hartree−Fock exchange is 100 at large interelectronic separation, but it is disconcerting that it is positive for all the other functionals.

III.C. Exciton Shift of TDDFT. One can assess the exciton shift in TDDFT by combining information about the response shift and the quasiparticle shift. For the GW100 data set, we have given the response shift in Figures 1 and 2 and the quasiparticle shifts in Figures 4 and 5 and Table 2. Figure 6 compares the hole shift and response shift to the exciton shift. The exciton shift is computed as the response shift minus the quasiparticle shift. Notice that the response shift used here is the same as the one shown in Figure 1b, and the quasiparticle shift used here is the same as the one in Figure 4a, which is obtained by comparing to the experimental data. Figure 6 shows that the exciton shift is surprisingly stable with respect to changing the percentage of Hartree−Fock exchange in the functional. Despite the various functional forms employed in the functionals in Table 1, the averaged exciton shift is in the narrow range of −4.8 to −5.1 eV.

How can we interpret this narrow range? We have defined the RS as the TDDFT excitation energy minus the orbital gap, and we have defined the QS as the experimental fundamental gap minus the orbital gap. Then we computed the ES as RS minus QS, which yields TDDFT excitation energy minus experimental fundamental gap. Since the latter is independent of the choice of functional (and hence independent of X), the variation represents simply the variation in the average TDDFT excitation energy, which, as we have shown in Figure 3, is very stable with respect to the percentage X employed in the functionals (much more stable than the orbital energy gap). Therefore, the near constancy (constant within 0.4 eV) of the lower curve in Figure 6 is simply a consequence of the fact that, averaged over all the transitions, the TDDFT excitation energy varies by only ∼0.4 eV. This is reasonable

https://dx.doi.org/10.1021/acs.jctc.0c00320
J. Chem. Theory Comput. 2020, 16, 4337−4350

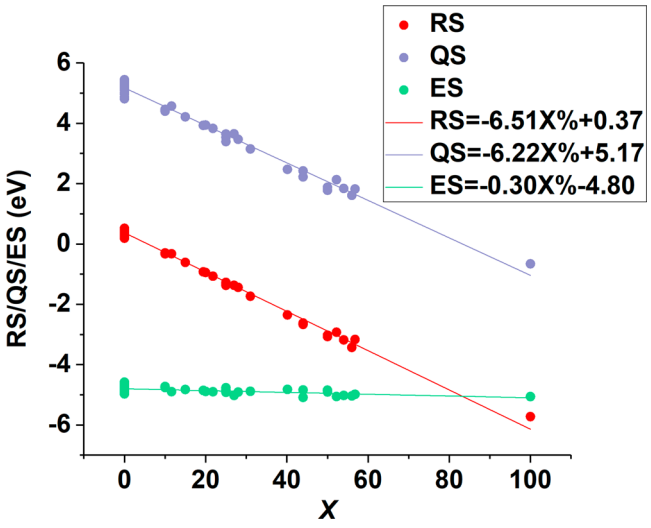

Figure 6. Response shift, quasiparticle shift, and exciton shift as a function of Hartree−Fock exchange in the functionals listed in Table 1 for the GW100 data set.

since most of the functionals are good to within ∼0.4 eV so their average cannot vary much more than that.

III.D. Generalized Response Shift in TDDFT. In the above discussion, we have limited our discussion to excitations, ionizations, and attachments involving only the HOMO and LUMO, and the languages of response shift, quasiparticle shift, and exciton shift are limited to HOMO (HOCO, or valence band maximum) and LUMO (LUCO, or conduction band minimum). Although this is sometimes enough for phenomenological discussions due to Kasha's rule,[100] a more detailed understanding of photoexcitation processes often requires consideration of higher excited states whose excitation character may be dominated by, for example, HOMO − 1 → LUMO or HOMO → LUMO + 1. The crystalline analogue of a HOMO − 1 → LUMO transition would be a transition from a state in the valence band that is not at the top of the valence band to a state at the bottom of the conduction band, and the quasiparticle hole associated with this transition is clearly different from the quasiparticle hole associated with the HOCO → LUCO transition. There is no well-established language for distinguishing the different holes; the present article is, however, focused on discussing molecular excitations, so from this point on, we use the language of molecules. For the quasiparticle concept to be useful, we must consider excitations that are dominated by a single independent-particle excitation, i.e., by a transition from the HOMO − m to the LUMO + n. We will call the orbital energy difference the (m,n) orbital energy interval. The difference in energy between the ionization potential when the HOMO − m electron is removed and the electron affinity in which an electron is added to the LUMO + n will be called the fundamental (m,n) interval, and the excitation energy associated with this transition will be called the optical (m,n) interval. Using the intervals rather than gaps, we can define three generalized shifts: the (m,n) quasiparticle shift, the (m,n) exciton shift, and the (m,n) response shift. The special cases of $(m,n) = (0,0)$ reverts back to the gaps.

With this language we can now extend our consideration to the (1,0) and (0,1) excitations. Specifically, we investigate the (1,0) response shift and (0,1) response shift in TDDFT for the VT28 data set. Figure 7 shows these generalized response shifts, and this figure shows that the generalized response shift is like the (0,0) one in having a strong correlation with the percentage of Hartree−Fock exchange.

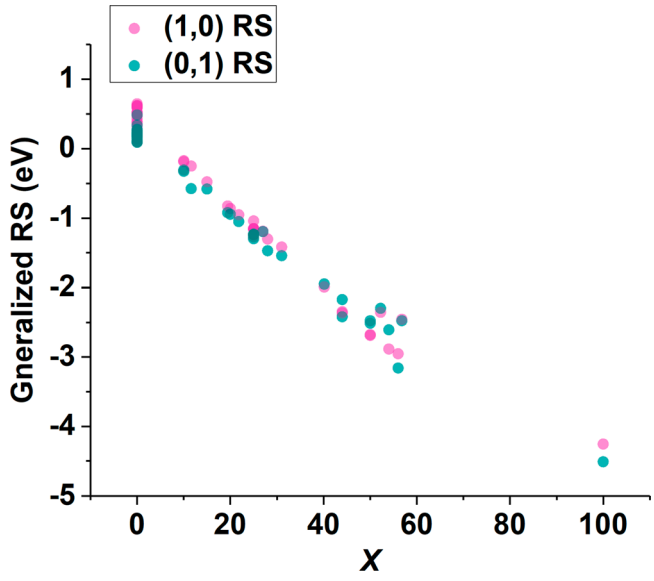

Figure 7. Generalized response shift as a function of percentage of Hartree−Fock exchange employed in the functionals for VT28 data set. The (1,0) response shift and (0,1) response shift are shown as pink and green dots, respectively.

IV. CONCLUDING REMARKS

The relationship between the Kohn−Sham orbital energy spectrum, the quasiparticle spectrum, and the optical spectrum raises many questions. Historically, Jones and Gunnarsson stated[101] that "The solution of the Dyson equation leads to the quasiparticle (QP) FS [Fermi surface], and the solution of the Kohn-Sham (KS) equation leads to a second, which we refer to as the KS-FS. It is a longstanding question whether the two surfaces, obtained using the exact self-energy and the exact exchange-correlation potential, respectively, are identical." We now know that they are not identical,[102] and the present study examined this kind of relationship, often discussed in the condensed-matter context, from a molecular point of view. By investigating three representative data sets, namely, the VT28, VT160, and GW100 sets, we found that the response shift in TDDFT (the difference between the quasiparticle gap and the optical gap) is drastically affected by the amount of Hartree−Fock exchange employed in density functionals. We can conclude that this effect is very general because of the diversity of the databases and functionals we employed; the databases include very different molecules, molecules at geometries other than the ground-state minimum, and excited states that are dominated by different characters, and the exchange-correlation functionals we examined have a variety of functional forms.

The response shift in TDDFT is negative for the most functionals but may be positive for local functionals or functionals with low (<10%) Hartree−Fock exchange. If interpreted physically in the quasiparticle picture, these positive response shifts would indicate a repulsive effect between the excited electrons and holes, which is the opposite of what one expects by Coulomb's law. The response shift changes linearly from about +1 eV to −5 eV as one increases the Hartree−Fock exchange from 0 to 100% in the density

https://dx.doi.org/10.1021/acs.jctc.0c00320
J. Chem. Theory Comput. 2020, 16, 4337−4350

functionals, yet the predicted excitation energies are accurate to an order of magnitude better than this range of response shifts. We conclude that one should not interpret the response shifts of functionals currently in practical use as physical effects (polarization or relaxation accompanying excitation, or screening), but rather, for most density functionals in common use (which are quite different from the unknown exact functional), we should interpret the orbital energies as mathematical intermediate quantities without a physical interpretation. We recommend that density functional calculations with currently available functionals should be interpreted in terms of their predictions of physical observables like fundamental gaps and optical gaps and not in terms of intermediate mathematical quantities like orbital energies (except for optimally tuned hybrids,[20] where by design the HOMO and LUMO should be taken seriously in terms of IP and EA).

As a side product, we found functionals with approximately 10% of Hartree−Fock exchange (the actual number obtained by linear regression is 9.7%) may yield an average response shift of zero. That means if one uses a functional with roughly 10% Hartree−Fock exchange, the obtained orbital energy gaps may resemble the molecular excitation energies.

The response shift is generalized beyond HOMO → LUMO transitions, and the generalized (0,1) and (1,0) response shifts are found to have a very similar behavior as a response shift in TDDFT. Although the response shift cannot be separated uniquely into a quasiparticle shift and exciton shift, we have assessed the quasiparticle shift and exciton shift by comparing the orbital energies to G_0W_0 quasiparticle energies as well as to experimental IPs, EAs, and FunGs. Our calculations show that the assessed quasiparticle shift is strongly dependent on the percentage of Hartree−Fock exchange employed in a functional. In fact, the required quasiparticle shift is the amount of energy required for the orbital gap to be equal to the fundamental gap. When compared to experimental fundamental gaps or G_0W_0 fundamental gaps, when Hartree−Fock exchange varies from 0 to 100%, the assessed quasiparticle shift may vary from 3.7 to −3.6 eV for the experimental comparison and from 5.2 to −1.1 eV for the G_0W_0 comparison. Such large variations of the difference of the KS orbital from the fundamental gap indicate that practical density functional approximations behave very differently from what is assumed in quasiparticle theory. Since the averaged experimental or G_0W_0 fundamental gaps do not depend on our choice of density functional, the small variation of the assessed exciton shift in fact represents the small variation of TDDFT excitation energies among the various functionals. As a result, the exciton shift calculated this way is relatively stable and is between −4.8 to −5.1 eV.

Why is the excitonic effect much larger in TDDFT for functionals with a larger Hartree−Fock exchange? For example, we observe functionals with 100% of Hartree−Fock exchange, e.g., PBEX with X = 100 and M06-HF, the response shift can reach −5 eV. In quantum chemistry language, one should think of the excitation as a process that involves both orbital relaxation and configuration interaction (of course for full CI, there is no need to consider the orbitals anymore). In solid-state physics language, one thinks of the excitation as a process that involves creation of an electron−hole pair (remove an electron from the valence band and create an electron in the conduction band) followed by electron−hole interaction. Usually, one employs GW to obtain accurate electron and hole energies, and the electron−hole interactions are described by BSE. One can think of the excitonic effect in TDDFT as including both the exciton binding energy and the quasiparticle shift for functionals with a larger Hartree−Fock exchange. Hence, the response shift in TDDFT is large for functionals with a large Hartree−Fock exchange.

AUTHOR INFORMATION

Corresponding Author

Donald G. Truhlar − *Department of Chemistry, Chemical Theory Center, and Minnesota Supercomputing Institute, University of Minnesota, Minneapolis, Minnesota 55455-0431, United States;* orcid.org/0000-0002-7742-7294; Email: truhlar@umn.edu

Author

Yinan Shu − *Department of Chemistry, Chemical Theory Center, and Minnesota Supercomputing Institute, University of Minnesota, Minneapolis, Minnesota 55455-0431, United States;* orcid.org/0000-0002-8371-0221

Complete contact information is available at: https://pubs.acs.org/10.1021/acs.jctc.0c00320

Notes

The authors declare no competing financial interest.

ACKNOWLEDGMENTS

The authors are grateful to Evert Jan Barerends, Leeor Kronik, and Mel Levy for helpful comments on a presubmission version of this article. This work was supported in part by the National Science Foundation under Grant CHE-1746186.

REFERENCES

(1) van Meer, R.; Gritsenko, O. V.; Baerends, E. J. Physical Meaning of Virtual Kohn-Sham Orbitals and Orbital Energies: An Ideal Basis for the Description of Molecular Excitations. *J. Chem. Theory Comput.* **2014**, *10*, 4432−4441.

(2) Janak, J. F. Proof that $\partial E/\partial n_i = \varepsilon_i$ in Density Functional Theory. *Phys. Rev. B: Condens. Matter Mater. Phys.* **1978**, *18*, 7165−7168.

(3) Perdew, J. P.; Parr, R. G.; Levy, M.; Balduz, J. L. Density-Functional Theory for Fractional Particle Number: Derivative Discontinuities of the Energy. *Phys. Rev. Lett.* **1982**, *49*, 1691−1694.

(4) Perdew, J. P.; Levy, M. Physical Content of the Exact Kohn-Sham Orbital Energies: Band Gaps and Derivative Discontinuities. *Phys. Rev. Lett.* **1983**, *51*, 1884−1887.

(5) Levy, M.; Perdew, J. P.; Sahni, V. Exact Differential Equation for the Density and Ionization Energy of a Many-Particle System. *Phys. Rev. A: At., Mol., Opt. Phys.* **1984**, *30*, 2745−2748.

(6) Levy, M.; Perdew, J. P. Hellmann-Feynman, Virial, and Scaling Requisites for the Exact Universal Density Functionals. Shape of the Correlation Potential and Diamagnetic Susceptibility for Atoms. *Phys. Rev. A: At., Mol., Opt. Phys.* **1985**, *32*, 2010−2021.

(7) Almbladh, C. O.; Pedroza, A. C. Density-Functional Exchange-Correlation Potentials and Orbital Eigenvalues for Light Atoms. *Phys. Rev. A: At., Mol., Opt. Phys.* **1984**, *29*, 2322−2330.

(8) Almbladh, C. O.; von Barth, U. Exact Results for the Charge and Spin Densities, Exchange-Correlation Potentials, and Density-Functional Eigenvalues. *Phys. Rev. B: Condens. Matter Mater. Phys.* **1985**, *31*, 3231−3244.

(9) Seidl, A.; Görling, A.; Vogl, P.; Majewski, J. A.; Levy, M. Generalized Kohn-Sham Schemes and the Band-Gap Problem. *Phys. Rev. B: Condens. Matter Mater. Phys.* **1996**, *53*, 3764.

(10) Perdew, J. P.; Levy, M. Comment on "Significance of the Highest Occupied Kohn-Sham Eigenvalue. *Phys. Rev. B: Condens. Matter Mater. Phys.* **1997**, *56*, 16021−16028.

(11) Politzer, P.; Abu-Awwad, F. A Comparative Analysis of Hartree-Fock and Kohn-Sham Orbital Energies. *Theor. Chem. Acc.* **1998**, *99*, 83−87.
(12) Stowasser, R.; Hoffmann, R. What Do the Kohn-Sham Orbitals and Eigenvalues Mean. *J. Am. Chem. Soc.* **1999**, *121*, 3414−3420.
(13) Chong, D. P.; Gritsenko, O. V.; Baerends, E. J. Interpretation of the Kohn-Sham Orbital Energies as Approximate Vertical Ionization Potentials. *J. Chem. Phys.* **2002**, *116*, 1760−1772.
(14) Grüning, M.; Marini, A.; Rubio, A. Density Functionals from Many-Body Perturbation theory: the Band Gap for semiconductors and Insulators. *J. Chem. Phys.* **2006**, *124*, 154108.
(15) Cohen, A. J.; Mori-Sánchez, P.; Yang, W. Fractional Charge Perspective on the Band Gap in Density-Functional Theory. *Phys. Rev. B: Condens. Matter Mater. Phys.* **2008**, *77*, 115123.
(16) Teale, A. M.; De Proft, F.; Tozer, D. J. Orbital Energies and Negative Electron Affinities from Density Functional Theory: Insight from the Integer Discontinuity. *J. Chem. Phys.* **2008**, *129*, 044110.
(17) Mori-Sánchez, P.; Cohen, A. J.; Yang, W. Localization and Delocalization Errors in Density Functional Theory and Implications for Band-Gap Prediction. *Phys. Rev. Lett.* **2008**, *100*, 146401.
(18) Korzdorfer, T.; Kummel, S.; Marom, N.; Kronik, L. When to Trust Photoelectron Spectra from Kohn-Sham Eigenvalues: The Case of Organic Semiconductors. *Phys. Rev. B: Condens. Matter Mater. Phys.* **2009**, *79*, 201205.
(19) Yang, W.; Cohen, A. J.; Mori-Sánchez, P. Derivative Discontinuity, Bandgap and Lowest Unoccupied Molecular Orbital in Density Functional Theory. *J. Chem. Phys.* **2012**, *136*, 204111.
(20) Kronik, L.; Stein, T.; Refaely-Abramson, S.; Baer, R. Excitation Gaps of Finite-Sized Systems from Optimally Tuned Range-Separated Hybrid Functionals. *J. Chem. Theory Comput.* **2012**, *8*, 1515−1531.
(21) Baerends, E. J.; Gritsenko, O. V.; van Meer, R. The Kohn-Sham Gap, the Fundamental Gap and the Optical Gap: the Physical Meaning of Occupied and Virtual Kohn-Sham Orbital Energies. *Phys. Chem. Chem. Phys.* **2013**, *15*, 16408−16425.
(22) van Aggelen, H.; Chan, G. K.-L. Single-Particle Energies and Density of States in Density Functional Theory. *Mol. Phys.* **2015**, *113*, 2018−2025.
(23) Proynov, E. Optimized Effective Potentials at a Glance: The Effective Exchange Potential of Becke−Johnson Applied to Molecules. *Theor. Chem. Acc.* **2016**, *135*, 248.
(24) Perdew, J. P.; Yang, W.; Burke, K.; Yang, Z.; Gross, E. K. U.; Scheffler, M.; Scuseria, G. E.; Henderson, T. M.; Zhang, I. Y.; Ruzsinszky, A.; Peng, H.; Sun, J.; Trushin, E.; Görling, A. Understanding Band Gaps of Solids in Generalized Kohn-Sham Theory. *Proc. Natl. Acad. Sci. U. S. A.* **2017**, *114*, 2801−2806.
(25) Perdew, J. P.; Ruzsinszky, A. Density-Functional Energy Gaps of Solids Demystified. *Eur. Phys. J. B* **2018**, *91*, 108.
(26) Baerends, E. J. Density Functional Approximation for Orbital Energies and Total Energies of Molecules and Solids. *J. Chem. Phys.* **2018**, *149*, 054105.
(27) Baerends, E. J. On Derivatives of the Energy with Respect to Total Electron Number and Orbital Occupation Numbers. A Critique of Janak'S Theorem. *Mol. Phys.* **2020**, *118*, e1612955.
(28) Godby, R. W.; Needs, R. J. Metal-Insulator Transition in Kohn-Sham Theory and Quasiparticle Theory. *Phys. Rev. Lett.* **1989**, *62*, 1169−1172.
(29) Onida, G.; Reining, L.; Rubio, A. Electronic Excitations: Density-Functional Versus Many-Body Green's-Function Approaches. *Rev. Mod. Phys.* **2002**, *74*, 601−659.
(30) Blase, X.; Duchemin, I.; Jacquemin, D. The Bethe-Salpeter Equation in Chemistry: Relations with TD-DFT, Applications and Challenges. *Chem. Soc. Rev.* **2018**, *47*, 1022−1043.
(31) Hohenberg, P.; Kohn, W. Inhomogeneous Electron Gas. *Phys. Rev.* **1964**, *136*, B864−B871.
(32) Kohn, W.; Sham, L. J. Self-Consistent Equations Including Exchange and Correlation Effects. *Phys. Rev.* **1965**, *140*, A1133−A1138.
(33) Seidl, A.; Görling, A.; Vogl, P.; Majewski, J. A.; Levy, M. Generalized Kohn-Sham Schemes and the Band-Gap Problem. *Phys. Rev. B: Condens. Matter Mater. Phys.* **1996**, *53*, 3764−3774.
(34) Landau, L. D. The Theory of Fermi Liquid. *Sov. Phys. JETP* **1957**, *3*, 920−925.
(35) Marder, M. P. *Condensed Matter Physics*; Wiley: New York, 2000; p 462ff.
(36) Schrieffer, J. R. What is a Quasi-Particle? *J. Res. Natl. Bur. Stand., Sect. A* **1970**, *74A*, 537−541.
(37) Levy, M.; Zahariev, F. Ground-State Energy as a Simple Sum of Orbital Energies in Kohn-Sham Theory: A Shift in Perspective through a Shift in Potential. *Phys. Rev. Lett.* **2014**, *113*, 113002.
(38) Wooten, F. *Optical Properties of Solids*; Academic: New York, 1972.
(39) Hedin, L. New Method for Calculating the One-Particle Green's Function with Application to the Electron-Gas Problem. *Phys. Rev.* **1965**, *139*, A796−A823.
(40) Godby, R. W.; Schlüter, M.; Sham, L. J. Self-Energy Operators and Exchange-Correlation Potentials in Semiconductors. *Phys. Rev. B: Condens. Matter Mater. Phys.* **1988**, *37*, 10159−10175.
(41) Hybertsen, M. S.; Louie, S. G. Electron Correlation in Semiconductors and Insulators: Band Gaps and Quasiparticle Energies. *Phys. Rev. B: Condens. Matter Mater. Phys.* **1986**, *34*, 5390−5413.
(42) Martin, P. C.; Schwinger, J. Theory of Many-Particle Systems. I. *Phys. Rev.* **1959**, *115*, 1342−1373.
(43) Yarlagadda, B. S.; Csanak, G.; Taylor, H. S.; Schneider, B.; Yaris, R. Application of Many-Body Green's Functions to the Scattering and Bound-State Properties of Helium. *Phys. Rev. A.* **1973**, *7*, 146−154.
(44) Purvis, G. D.; Öhrn, Y. Atomic and Molecular Electronic Spectra and Properties from the Electron Propagator. *J. Chem. Phys.* **1974**, *60*, 4063−4069.
(45) Dyson, F. J. The S Matrix in Quantum Electrodynamics. *Phys. Rev.* **1949**, *75*, 1736−1755.
(46) Žmuidzinas, J. S. Self-Consistent Green's-Function Approach to the Electron-Gas Problem. *Phys. rev. B* **1970**, *2*, 4445−4460.
(47) Doll, J. D.; Reinhardt, W. P. Many-Body Green's Functions for Finite, Nonuniform Systems: Applications to Closed Shell Atoms. *J. Chem. Phys.* **1972**, *57*, 1169−1184.
(48) Strinati, G.; Mattausch, H. J.; Hanke, W. Dynamical Correlation Effects on the Quasiparticle Bloch States of a Covalent Crystal. *Phys. Rev. Lett.* **1980**, *45*, 290−294.
(49) Strinati, G. Dynamical Shift and Broadening of Core Excitons in Semiconductors. *Phys. Rev. Lett.* **1982**, *49*, 1519−1522.
(50) Salpeter, E. E.; Bethe, H. A. A Relativistic Equation for Bound-State Problems. *Phys. Rev.* **1951**, *84*, 1232−1242.
(51) Csanak, C.; Taylor, H. S.; Yaris, R. Green's Function Technique in Atomic and Molecular Physics. *Adv. At. Mol. Phys.* **1971**, *7*, 287−361.
(52) Strinati, G. Application of the Green's Functions Method to the Study of the Optical Properties of Semiconductors. *Riv. Nuovo Cimento* **1988**, *11*, 1−86.
(53) Rohl fing, M.; Louie, S. G. Electron-Hole Excitations in Semiconductors and Insulators. *Phys. Rev. Lett.* **1998**, *81*, 2312−2315.
(54) Jacquemin, D.; Duchemin, I.; Blase, X. Benchmarking the Bethe-Salpeter Formalism on a Standard Organic Molecular Set. *J. Chem. Theory Comput.* **2015**, *11*, 3290−3304.
(55) Ashcroft, N. W.; Mermin, N. D. *Solid State Physics*; Saunders: Philadelphia, PA, 1976; p 349f.
(56) Loos, P.-F.; Scemama, A.; Blondel, A.; Garniron, Y.; Caffarel, M.; Jacquemin, D. A mountaineering strategy to excited states: Highly accurate reference energies and benchmarks. *J. Chem. Theory Comput.* **2018**, *14*, 4360−4379.
(57) Loos, P.-F.; Galland, N.; Jacquemin, D. Theoretical 0−0 Energies with Chemical Accuracy. *J. Phys. Chem. Lett.* **2018**, *9*, 4646−4651.
(58) Marques, M. A. L.; Gross, E. K. U. Time-dependent Density Functional Theory. *Annu. Rev. Phys. Chem.* **2004**, *55*, 427−455.

https://dx.doi.org/10.1021/acs.jctc.0c00320
J. Chem. Theory Comput. 2020, 16, 4337−4350

(59) Burke, K.; Werschnik, J.; Gross, E. K. U. Time-Dependent Density Functional Theory: Past, Present, and Future. *J. Chem. Phys.* **2005**, *123*, 062206.
(60) Baer, R.; Kronik, L. Time-Dependent Generalized Kohn-Sham Theory. *Eur. Phys. J. B* **2018**, *91*, 170.
(61) Skone, J. H.; Govoni, M.; Galli, G. Self-Consistent Hybrid Functional for Condensed Systems. *Phys. Rev. B: Condens. Matter Mater. Phys.* **2014**, *89*, 195112.
(62) Zhan, C. G.; Nichols, J. A.; Dixon, D. A. Ionization Potential, Electron Affinity, Electronegativity, Hardness, and Electron Excitation Energy: Molecular Properties from Density Functional Theory Orbital Energies. *J. Phys. Chem. A* **2003**, *107*, 4184−4195.
(63) Verma, P.; Wang, Y.; Ghosh, S.; He, X.; Truhlar, D. G. Revised M11 Exchange-Correlation Functional for Electronic Excitation Energies and Ground-State Properties. *J. Phys. Chem. A* **2019**, *123*, 2966−2990.
(64) Garrick, R.; Natan, A.; Gould, T.; Kronik, L. Exact Generalized Kohn-Sham Theory for Hybrid Functionals. *ChemRxiv* **2019**, DOI: 10.26434/chemrxiv.8869460.v3.
(65) Williams, A. R.; von Barth, U. In *Theory of the Inhomogeneous Electron Gas*; Lundqvist, S., March, N. H., Eds.; Plenum: New York, 1983.
(66) Schreiber, M.; Silva-Junior, M. R.; Sauer, S. P. A.; Thiel, W. Benchmarks for Electronically Excited States: CASPT2, CC2, CCSD, and CC3. *J. Chem. Phys.* **2008**, *128*, 134110.
(67) Jacquemin, D.; Perpète, E. A.; Ciofini, I.; Adamo, C.; Valero, R.; Zhao, Y.; Truhlar, D. G. On the Performances of the M06 Family of Density Functionals for Electronic Excitation Energies. *J. Chem. Theory Comput.* **2010**, *6*, 2071−2085.
(68) Hehre, W. J.; Radom, L.; Schleyer, P. v. R.; Pople, J. A. *Ab Initio Molecular Orbital Theory*; Wiley: New York, 1986.
(69) Jacquemin, D.; Duchemin, I.; Blase, X. 0−0 Energies Using Hybrid Schemes: Benchmarks of TD-DFT, CIS(D), ADC(2), CC2, and BSE formalisms for 80 Real-Life Compounds. *J. Chem. Theory Comput.* **2015**, *11*, 5340−5359.
(70) Zhao, Y.; Truhlar, D. G. The M06 Suite of Density Functionals for Main Group Thermochemistry, Thermochemical Kinetics, Noncovalent Interactions, Excited States, and Transition Elements: Two New Functionals and Systematic Testing of Four M06-Class Functionals and 12 Other Functionals. *Theor. Chem. Acc.* **2008**, *120*, 215−241.
(71) Weigend, F.; Ahlrichs, R. Balanced Basis Sets of Split Valence, Triple Zeta Valence and Quadruple Zeta Valence Quality for H to Rn: Design and Assessment of Accuracy. *Phys. Chem. Chem. Phys.* **2005**, *7*, 3297−3305.
(72) van Setten, M. J.; Caruso, F.; Sharifzadeh, S.; Ren, X.; Scheffler, M.; Liu, F.; Lischner, J.; Lin, L.; Deslippe, J. R.; Louie, S. G.; Yang, C.; Weigend, F.; Neaton, J. B.; Evers, F.; Rinke, P. GW100: Benchmarking G_0W_0 for Molecular Systems. *J. Chem. Theory Comput.* **2015**, *11*, 5665.
(73) Perdew, J. P.; Burke, K.; Ernzerhof, M. Generalized Gradient Approximation Made Simple. *Phys. Rev. Lett.* **1996**, *77*, 3865−3868.
(74) Shao, Y.; Gan, Z.; Epifanovsky, E.; Gilbert, A. T. B.; Wormit, M.; Kussmann, J.; Lange, A. W.; Behn, A.; Deng, J.; Feng, X.; Ghosh, D.; Goldey, M.; Horn, P. R.; Jacobson, L. D.; Kaliman, I.; Khaliullin, R. Z.; Kus, T.; Landau, A.; Liu, J.; Proynov, E. I.; Rhee, Y. M.; Richard, R. M.; Rohrdanz, M. A.; Steele, R. P.; Sundstrom, E. J.; Woodcock, H. L.; Zimmerman, P. M.; Zuev, D.; Albrecht, B.; Alguire, E.; Austin, B.; Beran, G. J. O.; Bernard, Y. A.; Berquist, E.; Brandhorst, K.; Bravaya, K. B.; Brown, S. T.; Casanova, D.; Chang, C.; Chen, Y.; Chien, S. H.; Closser, K. D.; Crittenden, D. L.; Diedenhofen, M.; DiStasio, R. A.; Do, H.; Dutoi, A. D.; Edgar, R. G.; Fatehi, S.; Fusti-Molnar, L.; Ghysels, A.; Golubeva-Zadorozhnaya, A.; Gomes, J.; Hanson-Heine, M. W. D.; Harbach, P. H. P.; Hauser, A. W.; Hohenstein, E. G.; Holden, Z. C.; Jagau, T.; Ji, H.; Kaduk, B.; Khistyaev, K.; Kim, J.; Kim, J.; King, R. A.; Klunzinger, P.; Kosenkov, D.; Kowalczyk, T.; Krauter, C. M.; Lao, K. U.; Laurent, A. D.; Lawler, K. V.; Levchenko, S. V.; Lin, C. Y.; Liu, F.; Livshits, E.; Lochan, R. C.; Luenser, A.; Manohar, P.; Manzer, S. F.; Mao, S.; Mardirossian, N.; Marenich, A. V.; Maurer, S. A.; Mayhall, N. J.; Neuscamman, E.; Oana, C. M.; Olivares-Amaya, R.; O'Neill, D. P.; Parkhill, J. A.; Perrine, T. M.; Peverati, R.; Prociuk, A.; Rehn, D. R.; Rosta, E.; Russ, N. J.; Sharada, S. M.; Sharma, S.; Small, D. W.; Sodt, A.; Stein, T.; Stueck, D.; Su, Y.; Thom, A. J. W.; Tsuchimochi, T.; Vanovschi, V.; Vogt, L.; Vydrov, O.; Wang, T.; Watson, M. A.; Wenzel, J.; White, A.; Williams, C. F.; Yang, J.; Yeganeh, S.; Yost, S. R.; You, Z.; Zhang, I. Y.; Zhang, X.; Zhao, Y.; Brooks, B. R.; Chan, G. K. L.; Chipman, D. M.; Cramer, C. J.; Goddard, W. A.; Gordon, M. S.; Hehre, W. J.; Klamt, A.; Schaefer, H. F.; Schmidt, M. W.; Sherrill, C. D.; Truhlar, D. G.; Warshel, A.; Xu, X.; Aspuru-Guzik, A.; Baer, R.; Bell, A. T.; Besley, N. A.; Chai, J.; Dreuw, A.; Dunietz, B. D.; Furlani, T. R.; Gwaltney, S. R.; Hsu, C.; Jung, Y.; Kong, J.; Lambrecht, D. S.; Liang, W.; Ochsenfeld, C.; Rassolov, V. A.; Slipchenko, L. V.; Subotnik, J. E.; Van Voorhis, T.; Herbert, J. M.; Krylov, A. I.; Gill, P. M. W.; Head-Gordon, M. Adavances in Molecular Quantum Chemistry Contained in the Q-Chem 4 Program Package. *Mol. Phys.* **2015**, *113*, 184−215.
(75) Talman, J. D.; Shadwick, W. F. Optimized Effective Atomic Central Potential. *Phys. Rev. A.* **1976**, *14*, 36−40.
(76) Casida, M. E.; Huix-Rotllant, M. Progress in Time-Dependent Density-Functional Theory. *Annu. Rev. Phys. Chem.* **2012**, *63*, 287−323.
(77) Sai, N.; Barbara, P. F.; Leung, K. Hole Localization in Molecular Crystals from Hybrid Density Functional Theory. *Phys. Rev. Lett.* **2011**, *106*, 226403.
(78) Imamura, Y.; Kobayashi, R.; Nakai, H. Linearity Condition for Orbital Energies in Density Functional Theory (II): Application to Global Hybrid Functionals. *Chem. Phys. Lett.* **2011**, *513*, 130−135.
(79) Bylander, D. M.; Kleinman, L. Good Semiconductor Band Gaps with a Modified Local-Density Approximation. *Phys. Rev. B: Condens. Matter Mater. Phys.* **1990**, *41*, 7868−7871.
(80) Shimazaki, T.; Asai, Y. Band Structure Calculations Based on Screened Fock Exchange Method. *Chem. Phys. Lett.* **2008**, *466*, 91−94.
(81) Alkauskas, A.; Broqvist, P.; Pasquarello, A. Defect Levels through Hybrid Density Functionals: Insights and Applications. *Phys. Status Solidi B* **2011**, *248*, 775−789.
(82) Marques, M. A. L.; Vidal, J.; Oliveira, M. J. T.; Reining, L.; Botti, S. Density-Based Mixing $^{\text{Parame}}$ ter for Hybrid Functionals. *Phys. Rev. B: Condens. Matter Mater. Phys.* **2011**, *83*, 035119.
(83) Koller, D.; Blaha, P.; Tran, F. Hybrid Functionals for Solids with an Optimized Hartree-Fock Mixing Parameter. *J. Phys.: Condens. Matter* **2013**, *25*, 435503.
(84) Ferrari, A. M.; Orlando, R.; Rérat, M. Ab Initio Calculation of the Ultraviolet-Visible (UV-vis) Absorption Spectrum, Electron-Loss Function, and Reflectivity of Solids. *J. Chem. Theory Comput.* **2015**, *11*, 3245−3258.
(85) Chen, W.; Miceli, G.; Rignanese, G.-M.; Pasquarello, A. Nonempirical Dielectric-Dependent Hybrid Functional with Range Separation for Semiconductors and Insulators. *Phys. Rev. Mater.* **2018**, *2*, 073803.
(86) Cui, Z.-H.; Wang, Y.-C.; Zhang, M.-Y.; Xu, X.; Jiang, H. Doubly Screened Hybrid Functional: An Accurate First-Principles Approach for Both Narrow- and Wide-Gap Semiconductors. *J. Phys. Chem. Lett.* **2018**, *9*, 2338−2345.
(87) Brawand, N. P.; Vörös, M.; Govoni, M.; Galli, G. Generalization of Dielectric-Dependent Hybrid Functionals to Finite Systems. *Phys. Rev. X* **2016**, *6*, 041002.
(88) Zhao, Y.; Truhlar, D. G. Density Functionals with Broad Applicability in Chemistry. *Acc. Chem. Res.* **2008**, *41*, 157−167.
(89) Yanai, T.; Tew, D. P.; Handy, N. C. A New Hybrid Exchange-Correlation Functional Using the Coulomb-attenuating Method (CAM-B3LYP). *Chem. Phys. Lett.* **2004**, *393*, 51−57.
(90) Krukau, A. V.; Vydrov, O. A.; Izmaylov, A. F.; Scuseria, G. E. Influence of the Exchange Screening Parameter on the Performance of Screened Hybrid Functionals. *J. Chem. Phys.* **2006**, *125*, 224106.
(91) Henderson, T. M.; Janesko, B. G.; Scuseria, G. E. Generalized Gradient Approximation Model Exchange Holes for Range-Separated Hybrids. *J. Chem. Phys.* **2008**, *128*, 194105.

(92) Peverati, R.; Truhlar, D. G. Improving the Accuracy of Hybrid Meta-GGA Density Functionals by Range Separation. *J. Phys. Chem. Lett.* **2011**, *2*, 2810−2817.
(93) Peverati, R.; Truhlar, D. G. Screened-Exchange Density Functionals with Broad Accuracy for Chemistry and Solid-State Physics. *Phys. Chem. Chem. Phys.* **2012**, *14*, 16187−16191.
(94) Chai, J.-D.; Head-Gordon, M. Systematic Optimization of Long-Range Corrected Hybrid Density Functionals. *J. Chem. Phys.* **2008**, *128*, 084106.
(95) Mardirossian, N.; Head-Gordon, M. ωB97M-V: A Combinatorially Optimized, Range-Separated Hybrid, Meta-GGA Density Functional with VV10 Nonlocal Correlation. *J. Chem. Phys.* **2016**, *144*, 214110.
(96) Chai, J.-D.; Head-Gordon, M. Long-Range Corrected Hybrid Density Functionals with Damped Atom-Atom Dispersion Corrections. *Phys. Chem. Chem. Phys.* **2008**, *10*, 6615−6620.
(97) Lin, Y.-S.; Li, G.-D.; Mao, S.-P.; Chai, J.-D. Long-Range Corrected Hybrid Density Functionals with Improved Dispersion Corrections. *J. Chem. Theory Comput.* **2013**, *9*, 263−272.
(98) Mardirossian, N.; Ruiz Pestana, L.; Womack, J. C.; Skylaris, C.-K.; Head-Gordon, T.; Head-Gordon, M. Use of the rVV10 Nonlocal Correlation Functional in the B97M-V Density Functional: Defining B97M-rV and Related Functionals. *J. Phys. Chem. Lett.* **2017**, *8*, 35−40.
(99) Mardirossian, N.; Head-Gordon, M. ωB97X-V: A 10-Parameter, Range-Separated Hybrid, Generalized Gradient Approximation Density Functional with Nonlocal Correlation, Designed by a Survival-of-the-Fittest Strategy. *Phys. Chem. Chem. Phys.* **2014**, *16*, 9904−9924.
(100) Kasha, M. Characterization of Electronic Transitions in Complex Molecules. *Discuss. Faraday Soc.* **1950**, *9*, 14−19.
(101) Jones, R. O.; Gunnarsson, O. The density Functional Formalism, Its Applications and Prospects. *Rev. Mod. Phys.* **1989**, *61*, 689−746.
(102) Baerends, E. J. From the KS Band Gap to the Fundamental Gap in Solids. An Integer Electron Approach. *Phys. Chem. Chem. Phys.* **2017**, *19*, 15639.
(103) Stephens, P. J.; Devlin, F. J.; Chabalowski, C. F.; Frisch, M. J. Ab initio Calculation of Vibrational Absorption and Circular Dichroism Spectra Using Density Functional Force Fields. *J. Phys. Chem.* **1994**, *98*, 11623−11627.
(104) Lee, C.; Yang, W.; Parr, R. G. Development of the Colle-Salvetti Correlation-Energy Formula into a Functional of the Electron Density. *Phys. Rev. B: Condens. Matter Mater. Phys.* **1988**, *37*, 785−789.
(105) Becke, A. D. Density-Functional Thermochemistry. IV. Systematic Optimization of Exchange-Correlation Functionals. *J. Chem. Phys.* **1997**, *107*, 8554−8560.
(106) Mardirossian, N.; Ruiz Pestana, L.; Womack, J. C.; Skylaris, C.-K.; Head-Gordon, T.; Head-Gordon, M. Use of the rVV10 Nonlocal Correlation Functional in the B97M-V Density Functional: Defining B97M-rV and Related Functionals. *J. Phys. Chem. Lett.* **2017**, *8*, 35−40.
(107) Mardirossian, N.; Head-Gordon, M. Mapping the Genome of Meta-Generalized Gradient Approximation Density Functionals: The Search for B97M-V. *J. Chem. Phys.* **2015**, *142*, 074111.
(108) Becke, A. D. A New Mixing of Hartree-Fock and Local Density Functional Theories. *J. Chem. Phys.* **1993**, *98*, 1372−1377.
(109) Yu, H. S.; Zhang, W.; Verma, P.; He, X.; Truhlar, D. G. Nonseparable Exchange-Correlation Functional for Molecules, Including Homogeneous Catalysis Involving Transition Metals. *Phys. Chem. Chem. Phys.* **2015**, *17*, 12146−12160.
(110) Gáspár, R. Statistical Exchange for Electron in Shell and the Xα Method. *Acta Phys. Acad. Sci. Hung.* **1974**, *35*, 213−218.
(111) Vosko, S. H.; Wilk, L.; Nusair, M. Accurate Spin-Dependent Electron Liquid Correlation Energies for Local Spin Density Calculations: A Critical Analysis. *Can. J. Phys.* **1980**, *58*, 1200−1211.
(112) Boese, A. D.; Handy, N. C. A New Parametrization of Exchange-Correlation Generalized Gradient Approximation Functionals. *J. Chem. Phys.* **2001**, *114*, 5497−5503.
(113) Verma, P.; Truhlar, D. G. HLE16: A Local Kohn-Sham Gradient Approximation with Good Performance for Semiconductor Band Gaps and Molecular Excitation Energies. *J. Phys. Chem. Lett.* **2017**, *8*, 380−387.
(114) Zhao, Y.; Schultz, N. E.; Truhlar, D. G. Exchange-Correlation Functional with Broad Accuracy for Metallic and Nonmetallic Compounds, Kinetics, and Noncovalent Interactions. *J. Chem. Phys.* **2005**, *123*, 161103.
(115) Zhao, Y.; Schultz, N. E.; Truhlar, D. G. Design of Density Functionals by Combining the Method of Constraint Satisfaction with Parametrization for Thermochemistry, Thermochemical Kinetics, and Noncovalent Interactions. *J. Chem. Theory Comput.* **2006**, *2*, 364−382.
(116) Zhao, Y.; Truhlar, D. G. Density Functional for Spectroscopy: No Long-Range Self-Interaction Error, Good Performance for Rydberg and Charge-Transfer States, and Better Performance on Average than B3LYP for Ground States. *J. Phys. Chem. A* **2006**, *110*, 13126−13130.
(117) Zhao, Y.; Truhlar, D. G. A New Local Density Functional for Main-Group Thermochemistry, Transition Metal Bonding, Thermochemical Kinetics, and Noncovalent Interactions. *J. Chem. Phys.* **2006**, *125*, 194101.
(118) Zhao, Y.; Truhlar, D. G. Exploring the Limit of Accuracy of the Global Hybrid Meta Density Functional for Main-Group Thermochemistry, Kinetics, and Noncovalent Interactions. *J. Chem. Theory Comput.* **2008**, *4*, 1849−1868.
(119) Peverati, R.; Truhlar, D. G. M11-L: A Local Density Functional That Provides Improved Accuracy for Electronic Structure Calculations in Chemistry and Physics. *J. Phys. Chem. Lett.* **2012**, *3*, 117−124.
(120) Peverati, R.; Truhlar, D. G. An Improved and Broadly Accurate Local Approximation to the Exchange-Correlation Density Functional: The MN12-L Functional for Electronic Structure Calculations in Chemistry and Physics. *Phys. Chem. Chem. Phys.* **2012**, *14*, 13171−13174.
(121) Yu, H. S.; He, X.; Li, S.; Truhlar, D. G. MN15: A Kohn-Sham Global-Hybrid Exchange-Correlation Density Functional with Broad Accuracy for Multi-reference and Single- reference Systems and Noncovalent Interactions. *Chem. Sci.* **2016**, *7*, 5032−5051.
(122) Yu, H. S.; He, X.; Truhlar, D. G. MN15-L: A New Local Exchange-Correlation Functional for Kohn-Sham Density Functional Theory with Broad Accuracy for Atoms, Molecules, and Solids. *J. Chem. Theory Comput.* **2016**, *12*, 1280−1293.
(123) Zhao, Y.; Truhlar, D. G. Hybrid Meta Density Functional Theory Methods for Thermochemistry, Thermochemical Kinetics, and Noncovalent Interactions: The MPW1B95 and MPWB1K Models and Comparative Assessments for Hydrogen Bonding and van der Waals Interactions. *J. Phys. Chem. A* **2004**, *108*, 6908−6918.
(124) Adamo, C.; Barone, V. Exchange Functionals with Improved Long-Range Behavior and Adiabatic Connection Methods without Adjustable Parameters: The mPW and MPW1PW models. *J. Chem. Phys.* **1998**, *108*, 664−675.
(125) Burke, K.; Ernzerhof, M.; Perdew, J. P. The Adiabatic Connection Method: A Non-Empirical Hybrid. *Chem. Phys. Lett.* **1997**, *265*, 115−120.
(126) Peverati, R.; Truhlar, D. G. Exchange-Correlation Functional with Good Accuracy for Both Structural and Energetic Properties while Depending Only on the Density and Its Gradient. *J. Chem. Theory Comput.* **2012**, *8*, 2310−2319.
(127) Hoe, W.-M.; Cohen, J.; Handy, N. C. Assessment of a New Local Exchange Functional OPTX. *Chem. Phys. Lett.* **2001**, *341*, 319−328.
(128) Handy, N. C.; Cohen, A. J. Left−Right Correlation Energy. *Mol. Phys.* **2001**, *99*, 403−412.
(129) Adamo, C.; Barone, V. Toward Reliable Density Functional Methods Without Adjustable Parameters: The PBE0 Model. *J. Chem. Phys.* **1999**, *110*, 6158−6170.

https://dx.doi.org/10.1021/acs.jctc.0c00320
J. Chem. Theory Comput. 2020, 16, 4337−4350

(130) Bernard, Y. A.; Shao, Y.; Krylov, A. I. General Formulation of Spin-Flip Time-Dependent Density Functional Theory Using Non-collinear Kernels: Theory, Implementation, and Benchmarks. *J. Chem. Phys.* **2012**, *136*, 204103.
(131) Perdew, J. P.; Chevary, J. A.; Vosko, S. H.; Jackson, K. A.; Pederson, M. R.; Singh, D. J.; Fiolhais, C. Atoms, Molecules, Solids, and Surfaces: Applications of the Generalized Gradient Approximation for Exchange and Correlation. *Phys. Rev. B: Condens. Matter Mater. Phys.* **1992**, *46*, 6671−6687.
(132) Zhang, Y.; Yang, W. Comment on "Generalized Gradient Approximation Made Simple. *Phys. Rev. Lett.* **1998**, *80*, 890.
(133) Perdew, J. P.; Ruzsinszky, A.; Csonka, G. I.; Constantin, L. A.; Sun, J. Workhorse Semilocal Density Functional for Condensed Matter Physics and Quantum Chemistry. *Phys. Rev. Lett.* **2009**, *103*, 026403.
(134) Csonka, G. I.; Perdew, J. P.; Ruzsinszky, A. Global Hybrid Functionals: A Look at the Engine under the Hood. *J. Chem. Theory Comput.* **2010**, *6*, 3688−3703.
(135) Peverati, R.; Truhlar, D. G. A Global Hybrid Generalized Gradient Approximation to the Exchange-Correlation Functional that Satisfies the Second-Order Density Gradient Constraint and Has Broad Applicability in Chemistry. *J. Chem. Phys.* **2011**, *135*, 191102.
(136) Perdew, J. P.; Wang, Y. Accurate and Simple Analytic Representation of the Electron-Gas Correlation Energy. *Phys. Rev. B: Condens. Matter Mater. Phys.* **1992**, *45*, 13244−13249.
(137) Boese, A. D.; Handy, N. C. New Exchange-Correlation Density Functionals: The Role of the Kinetic-Energy Density. *J. Chem. Phys.* **2002**, *116*, 9559−9569.
(138) Grimme, S. Accurate Calculation of the Heats of Formation for Large Main Group Compounds with Spin-Component Scaled MP2 Methods. *J. Phys. Chem. A* **2005**, *109*, 3067−3077.
(139) Tao, J.; Perdew, J. P.; Staroverov, V. N.; Scuseria, G. E. Climbing the Density Functional Ladder: Nonempirical Meta-Generalized Gradient Approximation Designed for Molecules and Solids. *Phys. Rev. Lett.* **2003**, *91*, 146401.
(140) Staroverov, V. N.; Scuseria, G. E.; Tao, J.; Perdew, J. P. Comparative Assessment of a New Nonempirical Density Functional: Molecules and Hydrogen-Bonded Complexes. *J. Chem. Phys.* **2003**, *119*, 12129−12137.
(141) Xu, X.; Goddard III, W. A. The X3LYP Extended Density Functional for Accurate Descriptions of Nonbond Interactions, Spin States, and Thermochemical Properties. *Proc. Natl. Acad. Sci. U. S. A.* **2004**, *101*, 2673−2677.

https://dx.doi.org/10.1021/acs.jctc.0c00320
J. Chem. Theory Comput. 2020, 16, 4337−4350